

Supplementary material for: An ensemble of AMIP simulations with prescribed land surface temperatures

Duncan Ackerley^{1,2}, Robin Chadwick³, Dietmar Dommegget¹, and Paola Petrelli⁴

¹ARC Centre of Excellence for Climate System Science, School of Earth Atmosphere and Environment, Monash University, Clayton 3800, Victoria, Australia

²Met Office, Exeter, UK

³Met Office Hadley Centre, Exeter, UK

⁴ARC Centre of Excellence for Climate System Science, Institute for Marine and Antarctic Studies, University of Tasmania, Hobart, Tasmania, Australia

Correspondence: Duncan Ackerley (duncan.ackerley@metoffice.gov.uk)

Copyright statement. The works published in this journal are distributed under the Creative Commons Attribution 4.0 License. This licence does not affect the Crown copyright work, which is re-usable under the Open Government Licence (OGL). The Creative Commons Attribution 4.0 License and the OGL are interoperable and do not conflict with, reduce or limit each other.

© Author(s) and British Crown Copyright 2018

5 This supplementary information contains four figures:

- (1) The change in surface air temperature, precipitation and mean sea level pressure for each of the perturbed (SST+4K, 4xCO₂, 4xCO₂rad and solar+3.3%) AMIP free land simulations relative to the AMIP free land control run (Fig. S1) as a reference to show the climatic changes associated with each forcing.
- (2) The change in surface air temperature, precipitation and mean sea level pressure for each of the perturbed (SST+4K, 10 4xCO₂, 4xCO₂rad and solar+3.3%) AMIP prescribed land simulations relative to the AMIP prescribed land control run (Fig. S2) as a reference to show the climatic changes in the prescribed land experiments are comparable to those of their free land counterparts.
- (3) The change in surface latent heat flux over the Amazon for each free land simulation relative to its prescribed land counterpart to show the increases associated with the higher precipitation in the prescribed land simulations (Fig. S3).
- (4) The change in canopy water loading (kg m⁻²) taken from 116 instantaneous seasonal values (first day of each season over 29 years) from both the A_{PL} and A simulations (Fig. S4). The 116 values are taken from the model restart files as climatological averages were not retained during the simulation. The positive change in canopy water loading corresponds with both the higher precipitation (Fig. 1(h) in the main text) and latent heat fluxes (Fig. S3) that are seen in A_{PL} relative to A, which agrees with the physical mechanism proposed in Section 3.2.1 of the main text.

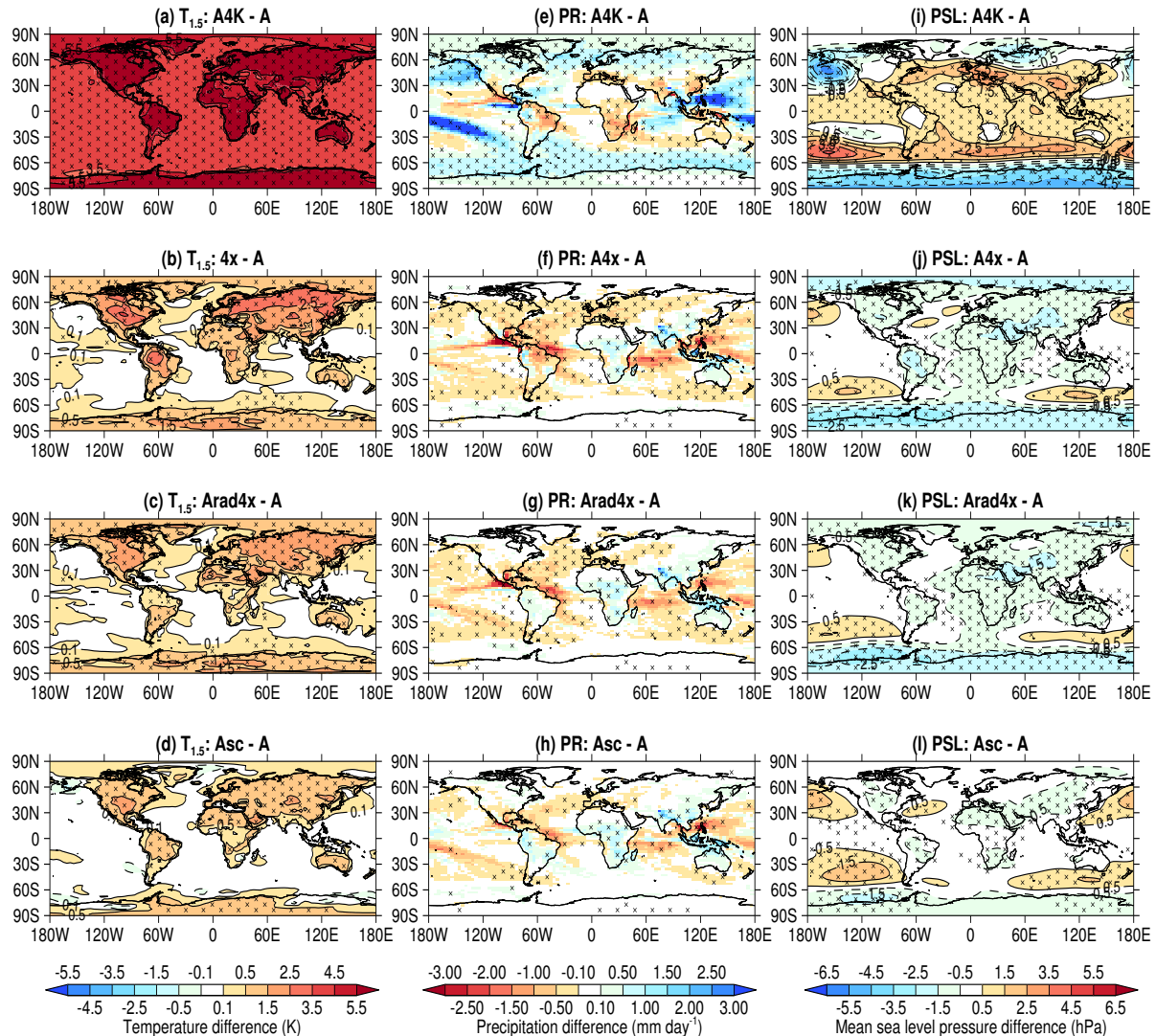


Figure S1. Differences in surface air temperature (TAS, K) for (a) A4K-A, (b) A4x-A, (c) Arad4x-A, (d) Asc-A. Equivalent differences between like-for-like simulations are given in (e)–(h) and (i)–(l) for precipitation (PR, mm day^{-1}) and mean sea level pressure (PSL, hPa), respectively. The points labelled with an "x" indicate the differences are statistically significant using the Student's t-test ($p \leq 0.05$).

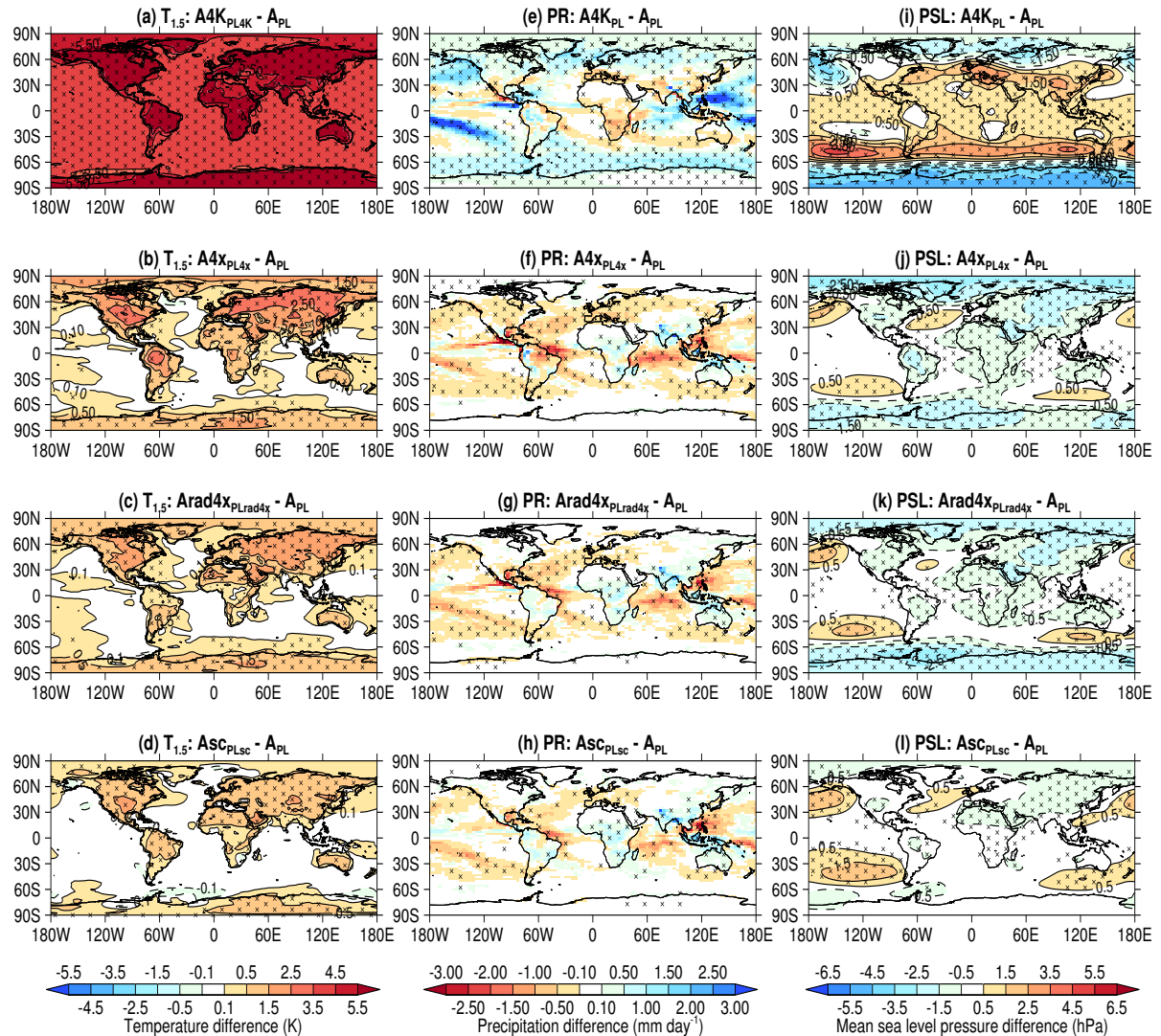


Figure S2. Differences in surface air temperature (TAS, K) for (a) A4K_{PL}4K - A_{PL}, (b) A4x_{PL}4x - A_{PL}, (c) Arad4x_{PLrad}4x - A_{PL}, (d) Asc_{PLsc} - A_{PL}. Equivalent differences between like-for-like simulations are given in (e)–(h) and (i)–(l) for precipitation (PR, mm day⁻¹) and mean sea level pressure (PSL, hPa), respectively. The points labelled with an "x" indicate the differences are statistically significant using the Student's t-test ($p \leq 0.05$).

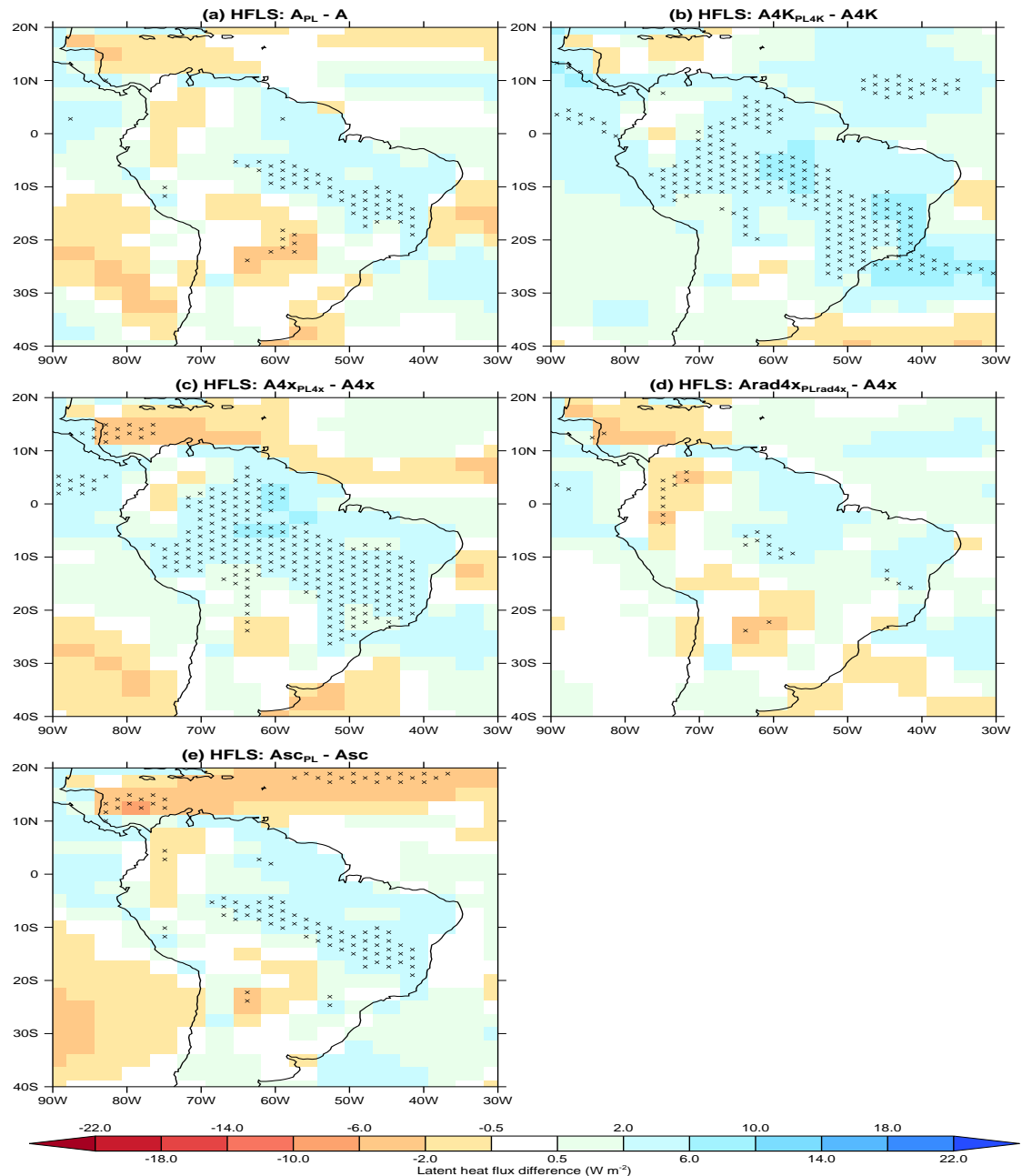


Figure S3. The difference in surface latent heat flux (W m^{-2}) for (a) A_{PL} - A , (b) $A4K_{PL4K}$ - $A4K$, (c) $A4x_{PL4x}$ - $A4x$, (d) $Arad4x_{PLrad4x}$ - $Arad4x$ and (e) Asc_{PL} - Asc . The points labelled with an "x" indicate the differences are statistically significant using the Student's t-test ($p \leq 0.05$).

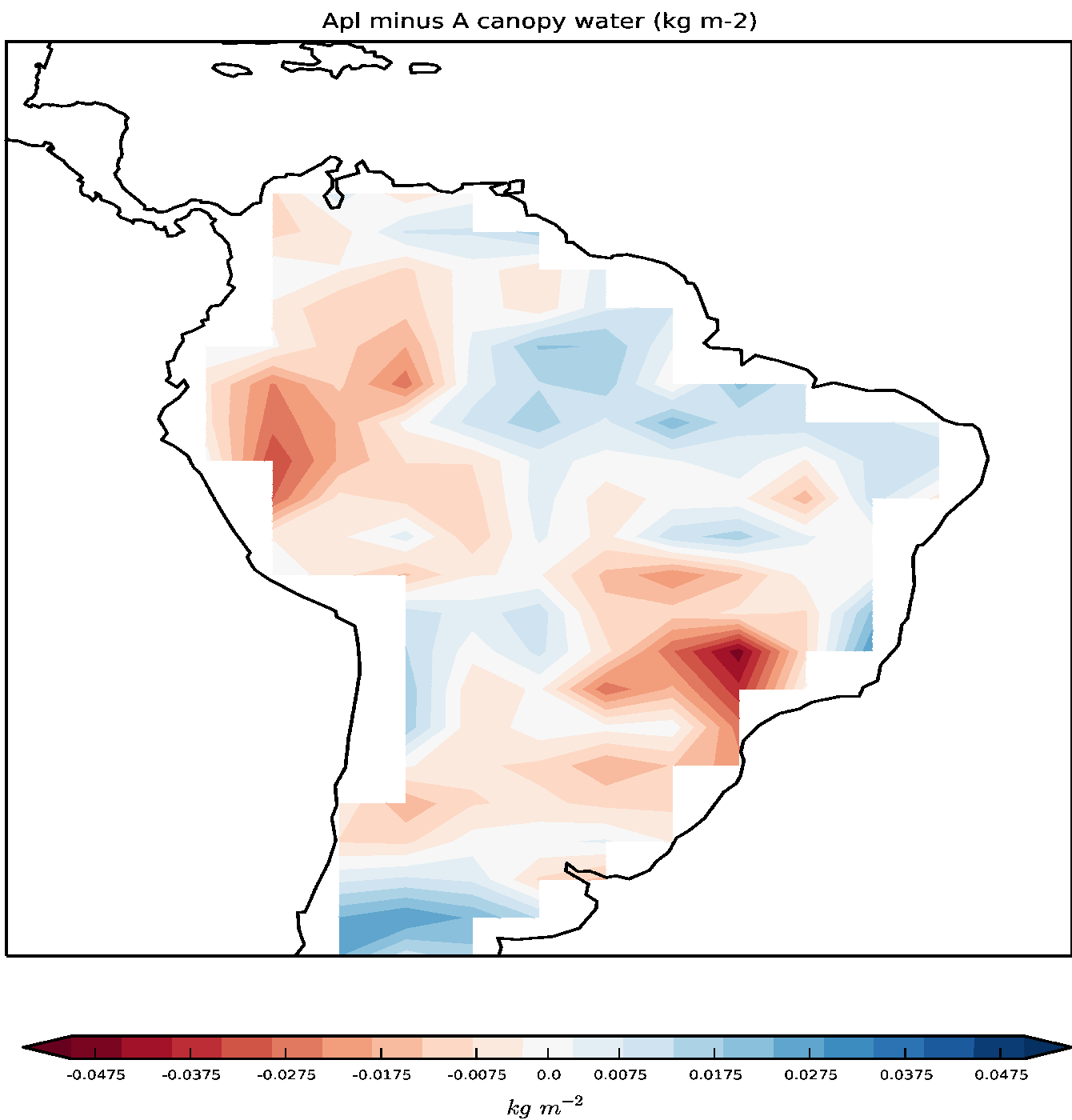


Figure S4. The difference in the canopy water loading (kg m^{-2}) in the *A_{PL}* simulation relative to *A*.